

Ultrafast polarization modulation in vertical cavity surface emitting lasers with frequency dependent current injection

A. V. Barve,¹ Y. Zheng,¹ L. Johansson,¹ A. Mehta,² A. Husain,² and L. Coldren¹

¹Department of Electrical and Computer Engineering, University of California, Santa Barbara, California 93117, USA

²Ziva Corporation, San Diego, California 92121, USA

(Received 15 October 2012; accepted 3 December 2012; published online 18 December 2012)

We report on a polarization modulation in vertical cavity surface emitting lasers (VCSEL), based on RF electrical injection. Complex polarization dynamics in the single mode regime is studied as a function of RF frequency and power at different bias currents. It has been observed that the polarization state of the VCSEL can be altered by changing the frequency of RF current modulation. Time resolved measurements show that by injecting periodic bursts of RF modulation in the VCSEL, it is possible to change the dominant polarization between the two orthogonal modes at gigahertz rates. © 2012 American Institute of Physics. [<http://dx.doi.org/10.1063/1.4772540>]

It is well known that vertical cavity surface emitting lasers (VCSEL) emit in one of the two orthogonal polarization modes.^{1,2} The polarization orientation in the lateral direction is hard to control due to the symmetric nature of typical VCSELs. Crystalline symmetries generally give rise to two dominant linear polarization directions, oriented along $\langle 110 \rangle$ and $\langle 1\bar{1}0 \rangle$ axes. The selection of one of the two linear polarization modes depends on various factors such as temperature, geometry, stress, location of cavity mode with respect the gain peak, and thus exhibit polarization switching at certain bias currents. Theoretical analysis of polarization properties of VCSELs has been carried out with rate equations that include the spin sublevels in conduction and valance bands.^{3,4} Various techniques have previously been used to control the polarization state of a VCSEL, such as, asymmetric current injection,⁵⁻⁷ controlled stress,⁸ electro-optic birefringence,⁹ which typically require more than two contacts per VCSEL or special packaging. Polarized optical injection is a popular method for dynamically controlling the state of polarization of a VCSEL, to create all optical polarization flip-flops.^{10,11} Although polarization switching up to 10 GHz has been demonstrated with this technique, it requires high speed optical pulses with two different polarizations, for set and reset switches. Polarization control through electrical injection is an attractive alternative. Although it is possible to control the state of the polarization by simply modulating the bias current,¹² it is a slow effect due to the thermal nature of the polarization switching process, with speeds limited to sub-MHz regimes.¹³ Current modulation experiments have been previously reported to analyze the nonlinear dynamics of VCSEL in gain switched regime,¹⁴ with observations of frequency doubling behavior.

In this letter, we introduce a technique for polarization modulation in VCSELs, with electrical RF frequency injection. It has been observed that it is possible to alter the power going into each polarization mode by simply varying the frequency of RF injection, while keeping all the other parameters, such as, bias current, temperature etc., the same. The polarized modulation response of VCSELs at several different bias currents and different modulation depths have been

measured to explore the complex nature of polarization modulation under these conditions. DC measurements, such as light power output-current-voltage (LIV) measurements and optical spectral measurements under these conditions confirm the power transfer in two different polarization modes as a function of RF frequency. Since this effect occurs at GHz frequencies, this polarization modulation is not driven by thermal effects and therefore can be extremely fast. To estimate the speed of the polarization modulation with this effect, VCSELs have been subjected to high speed bursts of electrical RF injection, and their polarized output have been measured in the time domain. These measurements reveal that this effect leads to fast modulation of polarization between X and Y polarized modes, above 1 GHz frequencies, which is more than an order of magnitude faster than other electrical injection techniques to control the polarization of a VCSEL.

VCSELs used for these measurements have a highly strained InGaAs/GaAs quantum-well (QW) active region, for 1060 nm operation. These VCSELs were grown on (100) semi-insulating GaAs substrates using a molecular beam epitaxy (MBE) system. The bottom mirror consisted of 18 periods of unintentionally doped (UID) GaAs/AlAs distributed Bragg reflectors (DBR), followed by a 1.75λ thick layer of Si doped GaAs to form an intracavity n-contact layer. The tapered oxide aperture layer was 0.5λ thick and was placed so that the tip of the taper occurs at the standing wave null. Four periods of deep oxidation layers are grown after that to reduce the capacitance. The p-type top mirror consists of GaAs/AlGaAs DBRs that are bandgap-engineered for low resistance and low optical loss. Details of this design can be found in Zheng *et al.*¹⁵ The active region is surrounded by an asymmetric $\text{Al}_{0.3}\text{Ga}_{0.7}\text{As}$ separate confinement heterostructure (SCH) that is parabolically graded down to GaAs spacers. Three 8 nm thick highly strained $\text{In}_{0.3}\text{Ga}_{0.7}\text{As}$ quantum wells are separated by 8 nm GaAs barriers, δ -doped with carbon using a carbon tetrabromide (CBr_4) precursor. The material was processed into circular-mesa VCSELs with varying diameters. The electrical and optical confinement was provided with tapered oxide apertures, with a total

oxidation length of $3\ \mu\text{m}$. The devices have a simple two contact geometry with a bottom emitting configuration. The substrate was coated with an antireflection (AR) layer of magnesium oxide (MgO) to avoid optical feedback.

Polarization sensitive LIV measurements on two $14\ \mu\text{m}$ mesa diameter devices, from different parts of the processed wafer are shown in Figs. 1(a) and 1(b). Polarization switching with high extinction ratio for single mode operation below the bias current of $1.4\ \text{mA}$, and a threshold current of $0.5\ \text{mA}$, was obtained. In both the devices (devices A and B), the dominant polarization mode changes from longer wavelength mode (Y-polarized) to shorter wavelength mode (X-polarized) (type I switching), and then back to longer wavelength mode (type II switching). However, these switching occur at different biases, as shown in Figs. 1(a) and 1(b). The difference in switching characteristics is due to nonuniformity during fabrication. All the devices tested showed a response similar to either device A or device B. For modulation response measurements, a RF signal from a high-speed network analyzer was injected into the VCSEL, on top of the DC bias current, using a bias-T. The light output from the VCSEL was then focused onto a 45° mirror, using an AR coated aspheric lens. A wire-grid polarizer was inserted in the beam path. The light was then coupled to a multimode fiber (MMF) using a second AR coated lens and detected using a high speed multimode detector. The electrical signal was amplified and fed back to the calibrated network analyzer to measure S_{21} , the electrical modulation transfer function of the VCSEL. The modulation transfer function was measured at several different DC biases and the resulting responses were plotted in two-dimensional contour plots, shown in Figs. 1(c)–1(f) for device A and Figs. 1(g)–1(j) for device B.

Figs. 1(c) and 1(d) show the response for X and Y polarizations in device A, for a nominal RF modulation amplitude of $-10\ \text{dBm}$, which corresponds to approximately $0.2\ \text{mA}$ peak to peak current variation in the VCSEL. Interestingly, at a bias current around $0.95\ \text{mA}$, there is a pronounced dip

in the frequency response of Y-polarized modulation, and a corresponding peak in X-polarized modulation response, near the relaxation resonance frequency. Results for device B at $-10\ \text{dBm}$ RF excitation are shown in Figs. 1(g) and 1(h) for X and Y polarizations, respectively. The nature of the modulation response curve changes as the RF modulation power is increased to $0\ \text{dBm}$ (approximately $0.60\ \text{mA}$ peak to peak current swing), as shown in Figs. 1(e) and 1(f) for device A and Figs. 1(i) and 1(j) for device B. For these powers, at bias currents higher than a polarization switching bias of $\sim 0.8\ \text{mA}$, significant modulation response is observed in both polarizations, which is very different than the DC behavior for a single-mode operation. It should be noted that these phenomena are not thermally driven, as the RF frequencies are much higher than typical thermal cutoff frequencies for polarization switching, which are less than $1\ \text{MHz}$.¹³

In order to verify that the actual power in different polarization modes is being varied, L-I-V measurements were carried out with the RF injection on. Fig. 2(a) shows the plot of LI curves at two different RF frequencies in both the polarizations for device B, for $5\ \text{dBm}$ RF excitation. Only the DC optical power is measured in this measurement. This shows the same trend as in Figs. 1(e), 1(f), 1(i), and 1(j), where the VCSEL starts emitting similar powers in both polarizations near the RF frequency of $2\text{--}4\ \text{GHz}$. For example, for $4\ \text{GHz}$ excitation, the VCSEL is emitting with similar powers in both the polarizations, until a bias current of $\sim 1.2\ \text{mA}$. This is in sharp contrast with the DC LIV curves shown in Figs. 1(a) and 1(b), as well as the L-I curve for $7\ \text{GHz}$ excitation. It should be noted that the current-voltage curve (not shown here) is identical for all the RF frequencies. Fig. 2(b) shows the optical spectrum measured at X and Y polarizations, for no RF excitation, and at $4\ \text{GHz}$ and $7\ \text{GHz}$ excitations at $1.05\ \text{mA}$ of DC bias. It is clear that for DC conditions with no RF injection, Y-polarized mode (longer wavelength mode) is $23\ \text{dB}$ higher than the X-polarized

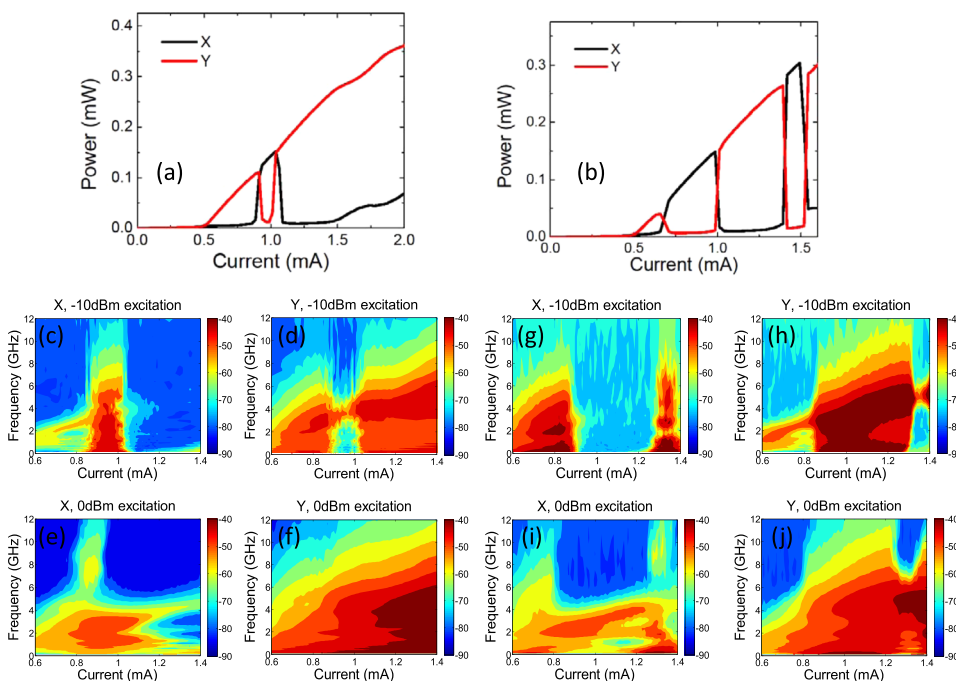


FIG. 1. Polarized optical power versus bias current curves for (a) device A and (b) device B. Polarization dependent modulation response as a function of bias for device A is plotted in (c) and (d) for X and Y polarization, respectively, for $-10\ \text{dBm}$ excitation. (e) and (f) show the corresponding curves for $0\ \text{dBm}$ modulation. (g)–(j) show the corresponding plots for device B, with $-10\ \text{dBm}$ and $0\ \text{dBm}$ modulation powers.

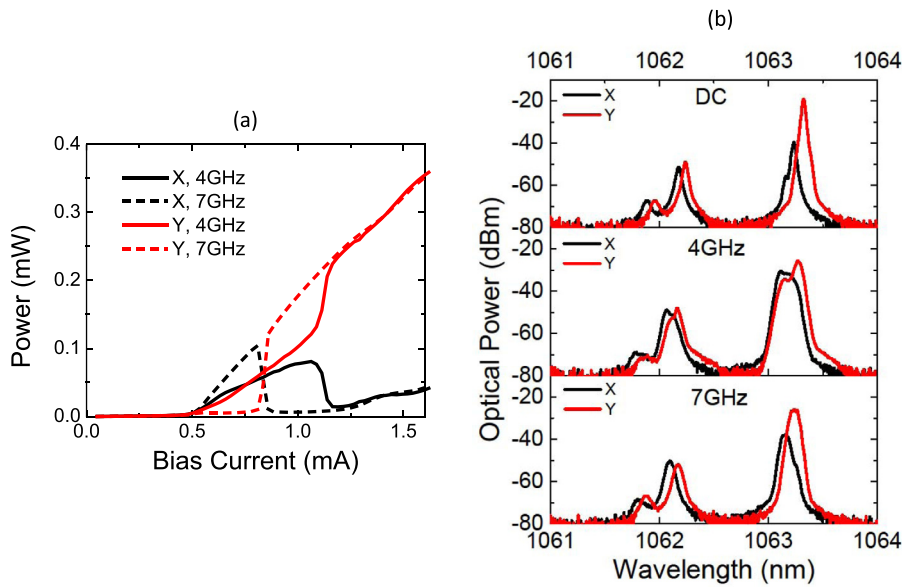


FIG. 2. Frequency dependent DC measurements for device B, showing (a) polarized L-I curves, at two different frequencies and (b) Polarized optical spectra.

mode at 1.05 mA. However, for RF excitation at 4 GHz, both the modes show nearly equal output. The Y-polarized mode starts dominating again as the frequency is increased further, with a 12 dB higher power than the X-polarized mode at 7 GHz RF frequency, at 1.05 mA. This measurement confirms that the power going into each polarization mode can be varied by simply changing the frequency of RF excitation.

To estimate the speed of the polarization modulation by changing the RF frequency or power, we set up a time domain polarization modulation measurement. The set up for the measurement is shown in Fig. 3. A constant frequency RF signal and a square wave are passed through a double-balanced mixer, to generate a gated RF signal. The inset in Fig. 3 shows an example of this mixing, with the green curve showing the square wave generated by a bit-rate generator and the black curve showing the gated RF signal. The small modulation in the “off” region is due to a small leakage of RF signal through the mixer. This gated RF signal is then applied across the VCSEL, along with a DC bias, with a bias-T circuit. The VCSEL output is passed through a

polarizer, then focused onto a MMF, detected with a high frequency detector, amplified and fed to an oscilloscope. A low pass filter is used to reduce the carrier RF signal by approximately 10 dB. The oscilloscope is synchronized to the square wave generator, but not with the RF generator, which results in varying phase of RF signal at the start of “on” region, as can be seen from the inset.

Fig. 4 shows the time domain response for X and Y polarized outputs at different modulation frequencies and bias currents with this configuration. The frequency of the RF source was kept constant at 4 GHz, and the modulation power was 5 dBm. Fig. 4(a) shows the response for a modulation frequency of 50 MHz. It is clear that the polarization mode changes from dominant X mode to dominant Y mode as we go from “on” to “off” state of the RF burst. The waveforms have been averaged in time to reduce the noise. This polarization modulation can be observed till much higher frequencies of the square wave. For example, Fig. 4(b) shows the response at 1.35 GHz square wave frequency at 1.05 mA of DC bias applied to the VCSEL. Output of X and Y channels are nearly 180° out of phase, indicating the

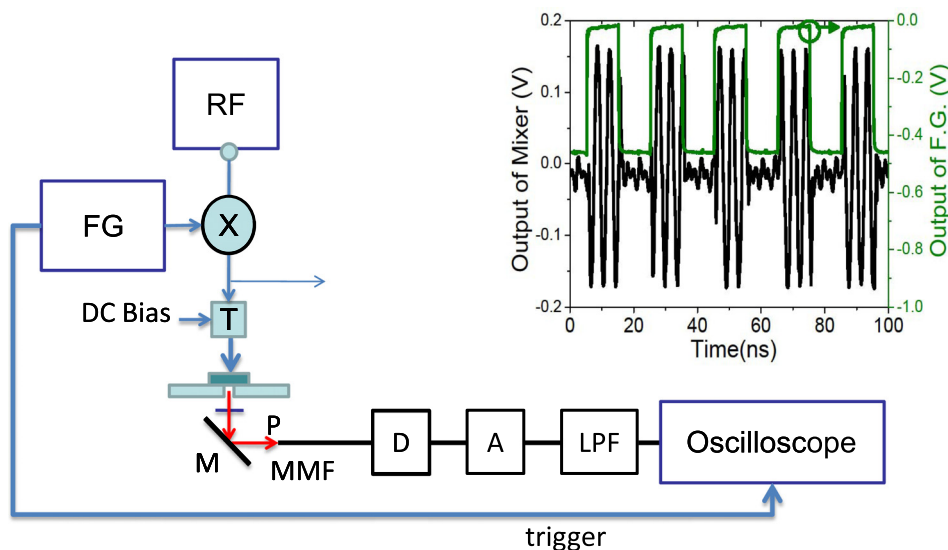


FIG. 3. Set up for time domain measurements. Different components are: RF—RF generator, FG—function generator for variable frequency square wave generation, X—frequency mixer, T—bias tee circuit, M—mirror, MMF—multi-mode optical fiber, P—polarizer, D—detector, A—amplifier, LPF—low pass filter. The inset shows the output of FG (green) and output of the mixer (black), showing periodic bursts of RF signal.

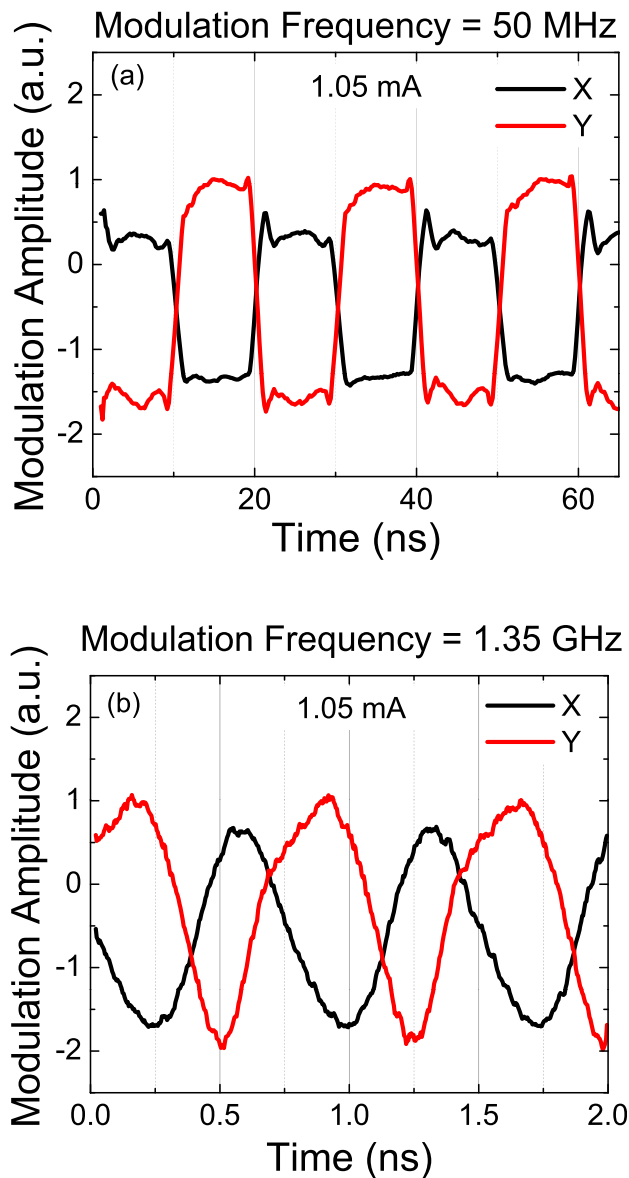


FIG. 4. Time domain modulation response for VCSEL in X and Y polarizations for modulation frequency of (a) 50 MHz, (b) 1.35 GHz at 1.05 mA bias current.

dominant polarization changing between the two modes, in less than 350 ps. This is, by far, the fastest reported polarization modulation using electrical injection. As the modulation frequency is increased further, the modulation frequency and RF frequency become comparable, and the modulation envelop is not clearly defined. Thus, it should be noted that the actual polarization modulation can be faster than the 1.35 GHz reported here. The high modulation frequencies

indicate that the polarization modulation is not caused by thermal effects.

In conclusion, a technique of electrically modulating the polarization of VCSELs is reported. By injecting the electrical RF signal into the VCSEL, the state of the polarization can be altered at high speeds. Polarized transfer function measurements at different modulation amplitudes reported here reveal complex polarization dynamics near the polarization switching point of a single mode VCSEL. These findings have been supported by optical spectral measurements and LIV measurements under various RF injection conditions. Time domain experiments reveal that polarization can be modulated by changing the RF frequency or power at speeds as high as 1.35 GHz.

This work was supported by DARPA, via STTR with Ziva Corp.

Disclaimer: The views expressed are those of the authors and do not reflect the official policy or position of the Department of Defense or the U.S. Government.

Distribution Statement "A" (Approved for Public Release, Distribution Unlimited).

¹G. Verschaffelt, K. Panajotov, J. Albert, B. Nagler, M. Peeters, J. Danckaert, I. Veretennicoff, and H. Thienpont (Association of Polish Electrical Engineers (SEP), 2001).

²K. D. Choquette, R. P. Schneider, K. L. Lear, and R. E. Leibenguth, *IEEE J. Sel. Top. Quantum Electron.* **1**(2), 661 (1995).

³M. San Miguel, Q. Feng, and J. V. Moloney, *Phys. Rev. A* **52**(2), 1728 (1995).

⁴J. Martin-Regalado, F. Prati, M. San Miguel, and N. B. Abraham, *IEEE J. Quantum Electron.* **33**(5), 765 (1997).

⁵L. M. Augustin, E. Smalbrugge, K. D. Choquette, F. Karouta, R. C. Strijbos, G. Verschaffelt, E. J. Geluk, T. G. van de Roer, and H. Thienpont, *IEEE Photon. Technol. Lett.* **16**(3), 708 (2004).

⁶Y. Zheng, C.-H. Lin, and L. A. Coldren, *IEEE Photon. Technol. Lett.* **23**(5), 305 (2011).

⁷Y. Sato, K. Furuta, T. Katayama, and H. Kawaguchi, *IEEE Photon. Technol. Lett.* **20**(17), 1446 (2008).

⁸K. Panajotov, B. Nagler, G. Verschaffelt, A. Georgievski, H. Thienpont, J. Danckaert, and I. Veretennicoff, *Appl. Phys. Lett.* **77**(11), 1590 (2000).

⁹M. S. Park, B. T. Ahn, B.-S. Yoo, H. Y. Chu, H.-H. Park, and C. J. Chang-Hasnain, *Appl. Phys. Lett.* **76**(7), 813 (2000).

¹⁰H. Kawaguchi, *Opto-Electron. Rev.* **17**(4), 265 (2009).

¹¹D. L. Boiko, G. M. Stephan, and P. Besnard, *J. Appl. Phys.* **86**(8), 4096 (1999).

¹²K. D. Choquette, K. L. Lear, R. E. Leibenguth, and M. T. Asom, *Appl. Phys. Lett.* **64**(21), 2767 (1994).

¹³G. Verschaffelt, J. Albert, B. Nagler, M. Peeters, J. Danckaert, S. Barbay, G. Giacomelli, and F. Marin, *IEEE J. Quantum Electron.* **39**(10), 1177 (2003).

¹⁴K. Panajotov, I. Gatara, A. Valle, H. Thienpont, and M. Sciamanna, *IEEE J. Quantum Electron.* **45**(11), 1473 (2009).

¹⁵Y. Zheng, C.-H. Lin, A. V. Barve, and L. A. Coldren, in *IEEE Photonics Conference IPC2012* (IEEE, 2012), pp. 131–132.